PROTEINS: Structure, Function, and Genetics 33:1–17 (1998)

RESEARCH ARTICLES

Analytical Shape Computation of Macromolecules: I. Molecular Area and Volume Through Alpha Shape

Jie Liang,[1,2] Herbert Edelsbrunner,[2] Ping Fu,[1] Pamidighantam V. Sudhakar,[1] and Shankar Subramaniam[1,3]*

[1]*National Center for Supercomputing Applications, University of Illinois at Urbana-Champaign, Urbana, Illinois*
[2]*Department of Computer Science, University of Illinois at Urbana-Champaign, Urbana, Illinois*
[3]*Beckman Institute for Advanced Science and Technology, Departments of Biochemistry, Molecular & Integrative Physiology, and Chemical Engineering, Center for Biophysics and Computational Biology, University of Illinois at Urbana-Champaign, Urbana, Illinois*

ABSTRACT **The size and shape of macromolecules such as proteins and nucleic acids play an important role in their functions. Prior efforts to quantify these properties have been based on various discretization or tessellation procedures involving analytical or numerical computations. In this article, we present an analytically exact method for computing the metric properties of macromolecules based on the alpha shape theory. This method uses the duality between alpha complex and the weighted Voronoi decomposition of a molecule. We describe the intuitive ideas and concepts behind the alpha shape theory and the algorithm for computing areas and volumes of macromolecules. We apply our method to compute areas and volumes of a number of protein systems. We also discuss several difficulties commonly encountered in molecular shape computations and outline methods to overcome these problems. Proteins 33:1–17, 1998.**

Key words: solvent accessible surface; molecular surface; area and volume; Delaunay complex; alpha shape

INTRODUCTION

Macromolecules such as proteins and nucleic acids have complex structures. The specific spatial configurations of molecules are important for protein and nucleic acid function. The surface area and molecular volume are geometric quantities that determine various properties of these complex molecules. They play a role in protein folding,[1] conformational stability,[2] solubility,[3,4] crystal packing,[5,6] molecular recognition and docking,[7] and enzyme catalysis.[8] Recently, energy refinement methods have been developed which include the surface area[9] or excluded volume[10] for calculating solvation energies. With the advances in X-ray crystallography and NMR techniques, structures have been determined for many proteins and nucleic acids in atomic detail. Current and future structural results provide rich material for atomic-level molecular modeling and analysis.

Lee and Richards[11] introduced the models of solvent accessible surface (SA) and molecular surface (MS) for proteins. The molecular volume obtained from the MS model is also called the solvent excluded volume.[12] In the important special case of a point-sized solvent, the two surfaces are the same and referred to as the van der Waals surface (VW) of the molecule (see Fig. 1). These surface models provide a means to unambiguously define geometric properties of molecules and they motivate the development of algorithms and software for computing such properties. Computation of the surface area and volume of molecules has been the focus of research for some time, and algorithms of both analytical and numerical nature are available. In general, however, it is still difficult to rigorously and precisely describe and manipulate various aspects of the shape of a macromolecule.

The field of computational geometry has experienced rapid progress since its establishment in the late 70s[13,14] and some developments have direct

Grant sponsor: NSF; Grant numbers: ASC 94-04900, ASC 92-00301, ASC 89-02829, MCB 92-19619, and DBI 96-04223; Grant sponsor: ONR; Grant number: N00014-95-1-0692.

Jie Liang's current address is Department of Cheminformatics, SmithKline Beecham Pharmaceuticals, PO Box 1539, UW2940, 709 Swedeland Road, King of Prussia, PA 19406.

*Correspondence to Shankar Subramaniam, Beckman Institute for Advanced Science and Technology, Departments of Biochemistry, Molecular & Integrative Physiology, and Chemical Engineering, Center for Biophysics and Computational Biology, University of Illinois at Urbana-Champaign, Urbana, IL 61801. E-mail: shankar@ncsa.uiuc.edu

Received 3 September 1996; Accepted 7 April 1998

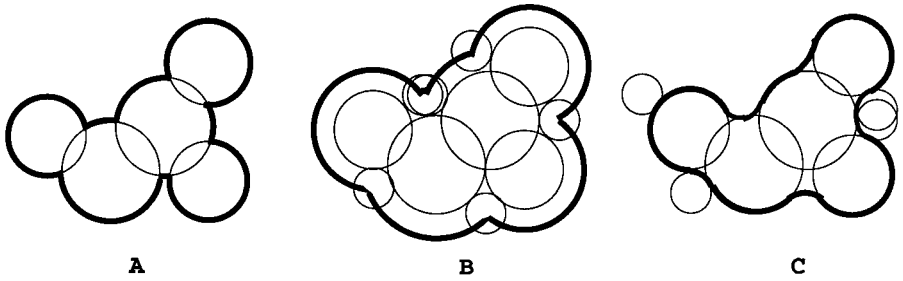

Fig. 1. Molecular surface models (**A**) van der Waals surface (VW), (**B**) solvent accessible surface (SA), and (**C**) molecular surface (MS).

implications for molecular biology. Among these, the alpha shape theory[15,17] provides a quantitative method to accurately describe and compute shapes at multilevels of detail in three-dimensional space. It uses Delaunay complexes and their filtrations to describe the topological structure of a molecule. The mathematical relationship between alpha shapes and the sphere models of a molecule has been firmly established.[16] With the availability of three-dimensional alpha shape software,[17,18,19] it is now possible to accurately and efficiently compute a variety of geometric aspects of molecules.

Computational methods to determine the area and volume based on VW, SA, and MS models can be broadly divided into two categories: approximation methods[20–29] and analytic methods.[10,12,12,30–35] Most approximation methods involve certain discretizations, such as polyhedral or triangular decompositions or the representation of a surface with a large number of dots. Among these methods, Richards' VOLUME program[21] is widely used and is distributed in the VADAR package.[36] It uses either bisector planes or planes based on van der Waals radii to divide the space of the internal atoms into polyhedra. Atoms on the surface are divided similarly with the help of fictitiously placed solvent atoms. The area and volume of the molecule are then calculated through these polyhedra. The GEPOL program, distributed as part of the ARVOLMOL package,[37] is one of the two programs known to us that compute both the MS area and volume.[27,38,39] It fills the solvent inaccessible space between atoms with spheres, and then triangulates these spheres. The triangles facing outside are selected and used in turn to compute area and volume.

Representing atoms by spherical balls provides the opportunity for analytic treatment of surface area and volume of molecules. Among the analytic methods, the ANAREA program distributed in the VADAR package computes the area of the SA model.[32] The MSDOT program by Connolly, which is distributed as part of ARVOMOL, is the second program computing the MS area and volume.[30,31,37] Closed-form analytical expressions for area and volume computation were also derived by Gibson and Sheraga;[33] they eliminate overlap of five or more atoms using an observation by Kratky.[40] In this article, we compare our results with those obtained using the programs ANAREA, GEPOL, MSDOT, and VOLUME.

First, we introduce the basic ideas and concepts behind the alpha shape theory as a fundamental approach to address geometric and topological questions about molecules. We then describe the alpha shape-based method for computing surface area and volume. We compare our computational results with results obtained by other methods. Finally, the appendices include details of the geometric and topological concepts and the computational aspects of our method.

THEORY AND ALGORITHMS

A full account of the alpha shape theory and the resulting algorithms for computing geometric properties of molecules can be found in computer science-oriented literature.[15–18] This article intuitively describes the most basic concepts and ideas behind the alpha shape theory, and provides more details in the appendix. It also explains the algorithms that compute the area and volume of a molecule based on its alpha complex.

Voronoi Diagram and Delaunay Complex

Three definitions of surface are widely used for molecular modeling. In each case, atoms are treated as intersecting spherical balls.[5,11,30] The *van der Waals surface* (VW) is the surface of what is covered by the atoms, each atom represented by a spherical ball of its van der Waals radius (Fig. 1A). The *solvent accessible surface* (SA) is generated by the center of the solvent (modeled as a rigid sphere) when rolling about the van der Waals surface of the molecule (Fig. 1B). The *molecular surface* (MS) is the surface generated by the front of the same solvent sphere (Fig. 1C).

In early work on algorithms for surface area computation, Richards and others applied Voronoi diagrams to decompose a molecule.[21,41,42] The Voronoi diagram divides the space into Voronoi regions, one per atom. A Voronoi region is generated by an atom, and consists of the part of space closest to this atom.[43] (When atoms with different radii are considered, the appropriate diagram is the weighted Voronoi diagram, also called the power diagram.) The boundaries of the Voronoi regions neatly divide up the entire molecule. The part of an atom contained in a Voronoi region has a simple shape which is always convex. Intuitively, we can sense that the Voronoi

diagram contains information about nearness among the atoms, since each Voronoi region is closest to its generating atom. A variety of applications of Voronoi diagrams to biology and chemistry have been published.[44,45]

The Delaunay complex is a geometric construct that can be derived from the Voronoi diagram by the following direct translation. The center of an atom ball with a Voronoi region becomes a vertex in the Delaunay complex. If two Voronoi regions share a common facet, then the edge connecting the centers of the two corresponding atom balls is in the complex. If three Voronoi regions share a common edge, then the triangle spanned by the three ball centers is in the complex. Finally, if four Voronoi regions share a common point, then the tetrahedron spanned by the four ball centers is in the complex. We have thus accounted for all possible intersection patterns among Voronoi regions, since in three-dimensional space there can be no more than four Voronoi regions that meet. The vertices, edges, triangles, and solid tetrahedra together form a special complex, called the *Delaunay complex*.[48] Recently, protein structures have been analyzed statistically in terms of Delaunay tetrahedra, where each amino acid residue is represented by a point placed at the C_α position. The results have been applied to sequence-based protein fold recognition.[49–51]

The Voronoi diagram and the Delaunay complex have very different appearances. For example, the Voronoi regions of the surface atoms may be unbounded and extend to infinity, whereas the whole Delaunay complex is bounded and lives within the convex hull of the atom centers. Nevertheless, these two geometric constructs are mathematically dual to one another. Both the Voronoi diagram and the Delaunay complex contain exactly the same combinatorial information (such as volume overlaps), although this information is represented differently. Therefore, we can obtain information about the Voronoi diagram by computing instead the corresponding Delaunay complex, which is easier than computing the Voronoi diagram. We use the DELCX program to compute the Delaunay complexes for molecules.[17,52,53] The algorithm used by DELCX has time-complexity O(n log n) when computing molecules, implying that the computing time required scales roughly to n log n, where n is the number of atoms.

Alpha Complexes and Alpha Shapes

The Delaunay complex of a molecule has many basic building blocks, i.e., vertex, edges, triangles, and tetrahedra, as described above. These basic building blocks are called *simplices*. We need to organize them rather than randomly pile them up. There is a natural way to arrange the simplices in a sequence.[17] It is based on a ball growth model and involves a parameter α that controls the growth of the balls. Essentially, the atom centers are swelled into balls of increasing radii as the controlling α value is increased. When two atom balls are large enough to touch one another, the edge connecting their centers appear. Similarly, when three or four atom balls are grown such that they meet at a common point, the triangle or tetrahedron spanning the atom centers appear, respectively. The "chronology" (alpha value) at which each of the basic elements in the Delaunay complex appears is then marked. In this way for a given value of α, simplices with this or smaller α value form a sequence (called a *simplicial complex*). More and more simplices of the Delaunay complex enter the sequence as α grows. When α becomes very large relative to the distances between atoms, the organized sequence contains all the simplices of the Delaunay complex. As a result, a parametric family of complexes and shapes are obtained from the Delaunay complex, and each reflects the shape accurately at a particular level of resolution.

The molecule with van der Waals atom radii is represented by the alpha complex when α is set to 0. This alpha complex retains the Delaunay tetrahedra, triangles, and edges that exactly correspond to overlapping atoms. Together with the Delaunay complex it contains a wealth of information about the spatial arrangement of the molecule. The key to making a connection to the actual molecule is to link the alpha complex with the Voronoi decomposition of the molecule, i.e., the restriction of the Voronoi diagram to the molecule (or, the intersection of the Voronoi diagram with the molecule). As demonstrated in Reference 16, the alpha complex reflects or encodes combinatorial, topological, and metric information about the molecule. Particularly, the alpha complex allows obtaining area and volume information directly from the alpha complex without explicitly constructing the geometric model of the molecule. As an application, we will see in this article and the companion article how the alpha complex can be translated into a combinatorial expression for the volume and surface area of a molecule and its cavities. An analytical method for identification and measurement of protein pockets has also been developed using alpha complex and discrete flow,[55] which has been applied to the pocket characterization of several proteins.[56,57]

COMPUTING AREA AND VOLUME

The computation of surface area and volume of a molecule has received much attention in the past. The problem is difficult because the spherical balls modeling the van der Waals atoms overlap due to chemical bonds, van der Waals contacts, and solvent contacts (when a solvent probe can touch two or more atoms simultaneously). Were the atoms completely isolated, we would only need to sum up the area and volume of each individual ball. An obvious approach is to use the principle of inclusion-exclusion: when two atoms overlap, we subtract the overlap, when

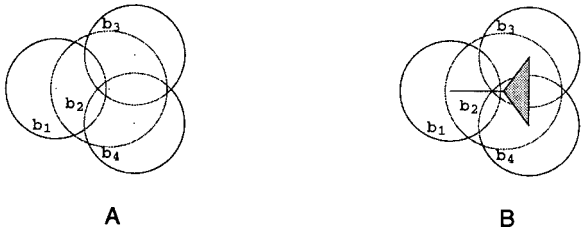

Fig. 2. Representation of the union of the atoms. (**A**) The application of the direct inclusion-exclusion formula. The alpha complex can be used to trim the list of terms from the straight application of the inclusion-exclusion principle. The resulting area formula contains only one term per simplex in the alpha complex. (**B**) The application of the short inclusion-exclusion formula, where the explicit computation of 3-degree overlap is avoided. (See text for details.)

three atoms overlap, we first subtract the pair overlaps, we then add back the triple overlap, etc. This continues when there are four, five, or more atoms intersecting. At a combinatorial level, the principle of inclusion-exclusion is related to the Gauss-Bonnet theorem used by Connolly.[30] It is still difficult to accurately keep track of where the overlaps occur, especially when there are many different combinatorial situations.[58]

Direct Inclusion-Exclusion

Once the alpha complex is constructed, it provides a route to untangling the combinatorial complexity of atom intersections. This is done by trimming the full inclusion-exclusion formula until it contains no redundant terms. An example of area computation by alpha shape trimmed inclusion-exclusion is shown in Figure 2. Let b_1, b_2, b_3, b_4 be the four disks. To simplify the notation we write A_i for the area of b_i, A_{ij} for the area of $b_i \cap b_j$, and A_{ijk} for the area of $b_i \cap b_j \cap b_k$. The total area of the union, $b_1 \cup b_2 \cup b_3 \cup b_4$, is

$$\begin{aligned} A_{total} = &(A_1 + A_2 + A_3 + A_4) \\ &- (A_{12} + A_{23} + A_{24} + A_{34}) \\ &+ A_{234}. \end{aligned}$$

We add the area of b_i if the corresponding vertex belongs to the alpha complex, we subtract the area of $b_i \cap b_j$ if the corresponding edge belongs to the alpha complex, and we add the area of $b_i \cap b_j \cap b_k$ if the corresponding triangle belongs to the alpha complex. This is an example of what we call the *direct inclusion-exclusion method*. Note that without the guidance of the alpha complex, the inclusion-exclusion formula may be written as

$$\begin{aligned} A_{total} = &(A_1 + A_2 + A_3 + A_4) \\ &- (A_{12} + A_{13} + A_{14} + A_{23} + A_{24} + A_{34}) \\ &+ (A_{123} + A_{124} + A_{134} + A_{234}) \\ &- A_{1234}. \end{aligned}$$

This contains six canceling redundant terms: $A_{13} = A_{123}$, $A_{14} = A_{124}$, and $A_{134} = A_{1234}$. Computing these terms would be wasteful. Such redundancy does not occur when we use the alpha complex: the part of the Voronoi regions contained in the respective atom balls for the redundant terms do not intersect. Therefore, the corresponding edges and triangles do not enter the alpha complex. In two dimensions, we have terms of at most three disk intersections, corresponding to triangles in the alpha complex. Similarly, in three dimensions the most complicated terms are intersections of four spherical balls, and they correspond to tetrahedra in the alpha complex.

It turns out that for three-dimensional molecules, intersections of five or more atom balls at a time can always be reduced to a "+" or "−" signed combination of intersections of four or fewer balls.[16] That overlaps of more than four balls actually occur for real molecular data and reductions are applicable is argued in Petitjean.[58] In particular, the union of all balls can be expressed as a signed combination of intersections, with a term per vertex, edge, triangle, tetrahedron in the alpha complex. Each vertex corresponds to a single ball taken positive, each edge corresponds to the intersection of two balls taken negative, each triangle corresponds to the intersection of three balls taken positive, and each tetrahedron corresponds to the intersection of four balls taken negative. In other words, following the combinatorial information of the alpha complex avoids higher order intersections altogether. Although the resulting formula is much smaller than the entire inclusion-exclusion formula, it expresses the exact volume and surface area of the molecule.[16] A further speed-up can be gained by using the *short inclusion-exclusion formula,* which is described in Appendix B2.

A brief description of the algorithmic implementation in the VOLBL package can be found in Appendix B. As illustrated in Figure 1, the combinatorial structure of the SA and the MS models of a molecule are the same. Both are represented by the same alpha complex. Therefore, we can also compute the area and volume of the MS model using the alpha complex (see Appendix for more details).

Checking Correctness

The program VOLBL has a built-in mechanism for checking the correctness of the computations. Using the checking option, it computes the surface area and volume of both SA and MS models by the direct and the short inclusion-exclusion formulas. After computing area and volume, the two results are checked to match to the last digit of precision. Besides checking the overall area and volume, VOLBL also checks the correctness of atomic SA contributions, which are again computed in two different ways and results are compared.

RESULTS

The protein structures for calculating area and volume are chosen from the protein databank and are listed in Table I. The computation based on alpha complexes involves four steps. The first step assigns the radii to the atom centers. The radius of an atom is its van der Waals radius plus the probe radius. When the radius of the probe is assigned to 0.0 Å by the utility program PDB2ALF, both the solvent accessible and molecular surface results will give the van der Waals area and volume. In these examples, van der Waals radii are taken from Richards' parameter set in VADAR. All accessible and molecular surface calculations use a probe radius of 1.2 Å. In the second step, the program DELCX computes the (weighted) Delaunay complex of the collection of atom balls, using the coordinates of the sphere centers and the radii as assigned by the first step. Its expected running time is on the order of n log n, where n is the number of atoms. Implicitly, DELCX also builds the (weighted) Voronoi diagram that decomposes the molecular space into non-overlapping convex pieces. The third step constructs the alpha complexes from the Delaunay complex using the program MKALF.[17] The running time is again on the order of n log n. The final step uses VOLBL to compute the metric area and volume, as well as the atomic contributions thereof. The SA and MS area and volume are computed simultaneously using one probe radius. All calculations are performed without corrections for the cusp condition. VOLBL requires time proportional to n. The constant of proportionality is relatively high so that the actual running time of VOLBL sometimes exceeds the time required for constructing the Delaunay complex and the alpha complexes, even for large proteins with tens of thousands of atoms. The actual running time for the short inclusion-exclusion version of VOLBL is significantly less than that for the direction inclusion-exclusion method. This is mostly due to the smaller constant of proportionality: only triplets rather than quadruplets of intersecting balls need to be considered. On an SGI workstation with an R5000 processor and 128 Mb memory, the timing for computing atomic volume and area of myoglobin (5mbn) is: 0.2 sec for PDB2ALF, 12.0 sec for DELCX, 24.3 sec for MKALF, 22.8 sec for VOLBL, and the overall time combined is 59.4 sec. This timing is for simultaneous area and volume (both SA and MS) computation, and between the two the volume computation is more time-consuming. In addition, DELCX generates the weighted Delaunay complex of the molecule, and MKALF generates a whole family of shapes with different α values. These can be further exploited for other calculations, e.g., analytical identification and measurement of pockets for binding sites and analysis of atomic nearest neighbor environment. Among those tested, GEPOL can also compute SA and MS volume. For myoglobin (5mbn), GEPOL takes 280.3 sec for a similar computation on the same machine. The MSDOT program, as bundled in Quantum Chemistry Program Exchange, does not compute volume (either SA or MS), and a direct comparison of timing is not possible. MSDOT takes 7.8 sec to compute the MS and SA surface area of myoglobin.

TABLE I. List of Proteins for Which Molecular Area and Volume Are Calculated

PDB name	# Res	Protein name	Reference
1eca	137	Hemoglobin (erythrocruorin, aquo met)	67
1nxb	62	Neurotoxin B	68
1rbc	124	Ribonuclease S mutant met13ala	69
1rbe	124	Ribonuclease S mutant met13phe	69
1rbf	124	Ribonuclease S mutant met13gly	69
1rbg	124	Ribonuclease S mutant met13ile	69
1rbh	124	Ribonuclease S mutant met13leu	69
1rbi	124	Ribonuclease S mutant met13val	69
2act	218	Actinidin	70
2cha	248	Alpha chymotrypsin a	71
2lyz	129	Lysozyme	72
2ptn	230	Trypsin	73
2rns	124	Ribonuclease S	74
2sn3	51	Scorpion neurotoxin	75
3cyt	104	Cytochrome C	76
3rn3	125	Ribonuclease A	77
4pti	58	Trypsin inhibitor	78
5mbn	154	Myoglobin (deoxy)	79
1arb	263	Achromobacter protease I	80
1cau	424	Canavalin	81
1cse	345	Subtilisin carlsberg	82
1ecd	136	Hemoglobin (erythrocruorin, deoxy)	67
1icm	131	Intestinal fatty acid binding protein	83
1mbd	153	Myoglobin (deoxy, pH 8.4)	84
1plc	99	Plastocyanin	85
1rro	108	Rat oncomodulin	86
1thm	279	Thermitase	87
1ycc	103	Cytochrome C	88
3sdh	292	Hemoglobin I	89
4gcr	174	Gamma-B crystallin	90
5p21	165	C-*H-Ras p21 protein	91

The computed areas for the proteins are given in Tables II, III, and IV. For comparison, VW, SA, and/or MS area are also computed using several programs distributed in the VADAR and ARVOMOL packages.[36,37] With the exception of VW volume, comparisons are given with the computations obtained with at least one analytical and one approximation method. From VADAR, VW volume is computed using Richards' VOLUME program (the bisection/radical plane method), and SA area is computed using Richmond's analytical ANAREA program. From ARVOMOL, VW, SA, and MS area and volume is computed using Pascual-Ahuir et al.'s

TABLE II. Computed van der Waals Surface (VW) Area (in Å^2) of Selected Proteins Using Alpha Shape Method VOLBL; Comparison With MS/MSDOT and GEPOL[27,30,31,37–39]

Protein	# Res	VOLBL	MS/ MSDOT	GEPOL
1eca	137	13852.0	13842.9	13909.4
1nxb	62	5673.7	5672.1	5683.3
1rbc	124	11996.6	11989.8	12040.3
1rbe	124	12060.9	12042.2	12120.8
1rbf	124	11960.8	11958.3	12025.2
1rbg	124	12054.2	12033.1	12106.8
1rbh	124	12061.2	12061.3	12160.8
1rbi	124	12047.7	12046.1	12102.7
2act	218	21252.3	21260.6	21162.0
2cha	248	22551.2	22521.6	22505.6
2lyz	129	12720.4	12700.7	12704.8
2ptn	230	21433.1	21439.9	21480.5
2rns	124	11853.0	11828.8	11867.7
2sn3	51	6453.6	6449.8	6432.4
3cyt	104	21158.1	21170.3	21125.1
3rn3	125	12332.2	12328.1	12287.9
4pti	58	5939.1	5939.4	5919.6
5mbn	154	16201.3	16192.0	16247.8
1arb	263	24796.8	24773.2	24861.1
1cau	424	37453.0	37452.7	37367.2
1cse	345	31905.9	31889.5	31955.6
1ecd	136	13826.2	13817.3	13862.2
1icm	131	14098.8	14108.9	14116.1
1mbd	153	16238.9	16220.5	16248.3
1plc	99	9726.1	9714.5	9760.0
1rro	108	11143.6	11144.1	11105.9
1thm	279	26174.1	26169.4	26123.8
1ycc	103	11152.2	11142.5	11102.6
3sdh	292	29941.1	29960.0	29981.6
4gcr	174	18900.2	18875.8	18893.9
5p21	165	17636.9	17611.3	17716.0

TABLE III. Computed Solvent Accessible (SA) Surface Area (in Å^2) of Selected Proteins Using Alpha Shape Method VOLBL; Comparison With ANAREA and GEPOL[27,32,37–39]

Protein	# Res	VOLBL	ANAREA	GEPOL
1eca	137	7085.2	7132.4	7111.1
1nxb	62	4035.3	4058.8	4027.7
1rbc	124	6679.0	6733.4	6721.7
1rbe	124	6619.4	6651.2	6618.2
1rbf	124	6624.6	6660.0	6661.8
1rbg	124	6619.4	6649.6	6581.7
1rbh	124	6628.7	6666.8	6647.4
1rbi	124	6607.0	6653.5	6573.8
2act	218	9157.4	9192.9	9131.5
2cha	248	10952.8	11073.1	10885.2
2lyz	129	6693.7	6765.6	6678.0
2ptn	230	9420.4	9463.6	9403.4
2rns	124	6635.9	6691.4	6669.7
2sn3	51	4198.6	4234.6	4183.9
3cyt	104	11634.8	11741.4	11633.5
3rn3	125	6857.6	6908.3	6814.9
4pti	58	3974.5	4019.6	3971.9
5mbn	154	8340.0	8433.3	8349.9
1arb	263	9707.9	9706.4	9733.9
1cau	424	20050.9	20171.5	20107.8
1cse	345	12729.4	12777.2	12718.8
1ecd	136	7056.6	7112.6	7089.8
1icm	131	7440.2	7519.5	7439.9
1mbd	153	8384.2	8500.9	8326.1
1plc	99	5056.5	5112.7	5044.8
1rro	108	5973.0	5999.7	5970.8
1thm	279	9879.2	9913.5	9873.9
1ycc	103	6498.8	6599.8	6372.7
3sdh	292	13674.3	13747.1	13695.4
4gcr	174	8918.8	8963.9	8974.2
5p21	165	8590.6	8639.4	8615.7

GEPOL program. VW and MS area are also computed using Connolly's analytical MS/MSDOT program.[37] In the calculations with GEPOL, we used 60 triangles to approximate an atom sphere. For consistency, all calculations use Richards' van der Waals radii parameter set available from the VADAR package[36] and a probe radius of 1.2 Å when SA or MS area/volume are computed.

Table II reports the VW surface area computed with the alpha shape-based analytical method, VOLBL, with Connolly's analytical method, MSDOT, and with Pascual-Ahuir et al.'s GEPOL method. Table III reports the SA areas computed with VOLBL, ANAREA, and GEPOL. Table IV reports the molecular surface area computed with VOLBL, MSDOT, and GEPOL. Tables V, VI, and VII compare results of volume computation using the alpha shape based VOLBL with results obtained with GEPOL and Richards' VOLUME. VOLBL and GEPOL compute volume in all three models, VW, SA, and MS, while Richards's VOLUME as distributed in VADAR only computes VW volume.

DISCUSSION

We see from Tables II, III, and IV that VW, SA, and MS area computed from VOLBL are comparable to the areas computed by other analytical methods such as ANAREA and MS/MSDOT. On the other hand, VW volumes computed with VOLBL and VOLUME differ significantly, with the latter giving volumes always larger by 20–40% (Table V). VOLUME is one of the earliest programs developed for molecular metric computation. This highlights the difference between the approximation and the analytic methods. Approximation methods are usually less accurate, because they do not rigorously deal with the complicated combinatorial problems of the molecular structures. To achieve faster speed, approximations are often made in these methods when errors are assumed to be tolerable, or when an accurate treatment is too involved or too costly. On the other hand, when fine-grained discretization is used and longer running times are allowed, the accuracy of approximation methods can converge to that of analytical methods.

TABLE IV. Computed Molecular Surface (MS) Area (in Å^2) of Selected Proteins Using Alpha Shape Method VOLBL; Comparison With MS/MSDOT and GEPOL[27,30,31,37–39†]

Protein	# Res	VOLBL	MS/ MSDOT	GEPOL
1eca	137	7002.0	6849.8	5970.7
1nxb	62	3437.1	3402.6	3196.5
1rbc	124	6070.9	5958.6	5337.0
1rbe	124	5921.0	5872.6	5341.5
1rbf	124	6003.5	5939.4	5351.0
1rbg	124	5917.1	5877.0	5380.4
1rbh	124	6017.6	5907.0	5391.6
1rbi	124	5914.9	5811.5	5389.1
2act	218	9135.2	8919.8	7740.7
2cha	248	11086.9	10796.4	9004.0
2lyz	129	6328.7	6248.6	5426.3
2ptn	230	9518.0	9380.5	7798.7
2rns	124	5836.0	5782.7	5375.6
2sn3	51	3572.6	3528.9	3316.3
3cyt	104	10895.4	10797.9	9796.3
3rn3	125	6089.5	6036.1	5601.3
4pti	58	3346.5	3346.0	3123.9
5mbn	154	8212.5	8048.0	6893.1
1arb	263	10009.3	9776.7	8177.7
1cau	424	20306.2	19855.6	16547.0
1cse	345	12649.5	12366.1	10592.0
1ecd	136	6948.5	6820.3	5888.2
1icm	131	7536.9	7390.0	6315.3
1mbd	153	8343.9	8152.8	6850.1
1plc	99	4387.0	4368.2	4114.6
1rro	108	5502.9	5379.5	4764.8
1thm	279	9692.5	9454.7	8228.1
1ycc	103	6060.4	5961.0	5292.8
3sdh	292	14037.1	13765.9	11731.4
4gcr	174	8634.1	8471.6	7381.9
5p21	165	8447.1	8202.3	7050.9

†The numbers for VOLBL reflect area without cusp correction, see Immersion of Molecular Surface.

TABLE V. Computed van der Waals Surface (VW) Volume (in Å^3) of Selected Proteins Using Alpha Shape Method VOLBL; Comparison With VOLUME and GEPOL[21,27,36–39]

Protein	# Res	VOLBL	VOLUME	GEPOL
1eca	137	13402.0	18740.1	13383.1
1nxb	62	5841.0	7522.3	5741.0
1rbc	124	11674.9	15693.2	11763.9
1rbe	124	11757.4	15512.2	11807.0
1rbf	124	11662.8	15679.4	11696.3
1rbg	124	11743.4	15793.4	11886.4
1rbh	124	11743.0	15795.0	11785.2
1rbi	124	11726.8	15763.4	11761.8
2act	218	20930.5	28303.9	21055.6
2cha	248	22431.3	31631.7	22460.5
2lyz	129	12663.4	17228.2	12594.1
2ptn	230	21031.0	29298.8	21305.9
2rns	124	11524.2	15400.9	11575.2
2sn3	51	6256.3	8410.9	6529.1
3cyt	104	20667.6	29345.1	20606.5
3rn3	125	12110.8	16279.2	12196.0
4pti	58	5836.5	7640.8	5830.2
5mbn	154	15816.5	22147.4	15944.2
1arb	263	24384.9	32636.1	24455.2
1cau	424	37337.7	52776.3	37335.9
1cse	345	31410.8	42659.3	31310.6
1ecd	136	13397.8	18768.5	13325.5
1icm	131	13579.7	19289.9	13519.3
1mbd	153	15835.4	22105.8	15764.2
1plc	99	9419.2	12580.7	9331.1
1rro	108	10687.6	14682.4	10769.9
1thm	279	25478.9	34946.0	25567.0
1ycc	103	10903.4	15162.8	10883.9
3sdh	292	29096.4	41242.6	28840.1
4gcr	174	18636.7	25478.9	18826.7
5p21	165	16987.1	23586.6	16998.0

Among the analytical methods, the difference in computed SA area between VOLBL and Richmond's ANAREA, as well as the difference in computed VW and MS area between VOLBL and Connolly's MS/MSDOT, are probably due to the (lack of) treatment of high order atom overlaps and different treatment of geometric degeneracy. We elaborate on both issues in the following two sections.

Higher Order Atom Overlap

Some of the available analytical methods ignore higher order overlaps of atoms. For example, it is reported that Connolly's analytical algorithm and related methods ignore overlaps of four or more atoms.[58] Petitjean [58] investigated this problem in detail. Using small molecules as examples, he discovered that the relative error can be around 30% for surface calculation and 5% for volume calculation when overlaps of four atoms and above are ignored. He also shows that in practical situations (e.g., aromatic compounds), overlaps of up to six atom balls occur frequently. Applications requiring high precision of surface area and volume computation should benefit from the use of VOLBL, which treats overlaps accurately.

Degeneracy

A fundamental issue in practical geometric computing is robustness; that is, whether programs crash or not. Common sources for the lack of robustness are geometric primitive tests that are ambiguous in degenerate or near degenerate cases. For example, degeneracy occurs when three or more points are collinear, when four or more points are coplanar, or when five or more points are cospherical. The trouble starts when a primitive geometric test is applied to these points. Different outcomes of such a test lead the process into logically different branches of the program. An arbitrary decision would typically be acceptable if it is consistent with earlier ones. However, inconsistent decisions can lead the program into geometrically impossible states that cannot be resolved.

TABLE VI. Computed Solvent Accessible (SA) Volume (in Å^3) of Selected Proteins Using Alpha Shape Method VOLBL; Comparison with GEPOL[27,37–39]

Protein	# Res	VOLBL	GEPOL
1eca	137	24932.8	25396.5
1nxb	62	11344.7	11273.0
1rbc	124	21919.6	21798.0
1rbe	124	21971.2	22040.4
1rbf	124	21839.0	21969.9
1rbg	124	21947.6	21819.7
1rbh	124	21941.3	21793.8
1rbi	124	21863.8	21890.7
2act	218	36890.6	36881.9
2cha	248	41058.5	40777.8
2lyz	129	23344.1	23540.1
2ptn	230	37563.5	37884.0
2rns	124	21667.5	21604.0
2sn3	51	12195.5	12112.7
3cyt	104	38715.6	38657.7
3rn3	125	22579.6	22433.7
4pti	58	11323.0	11067.5
5mbn	154	29316.7	29235.9
1arb	263	42314.7	42185.8
1cau	424	70369.1	70364.5
1cse	345	54619.0	54862.1
1ecd	136	24870.8	25504.8
1icm	131	25826.5	25898.8
1mbd	153	29354.5	29460.4
1plc	99	17391.9	17641.5
1rro	108	20034.6	19906.3
1thm	279	44096.1	43768.0
1ycc	103	20697.2	20240.6
3sdh	292	52726.6	52004.3
4gcr	174	33417.6	33776.8
5p21	165	31329.3	31251.5

TABLE VII. Computed Molecular Surface (MS) Volume (in Å^3) of Selected Proteins Using Alpha Shape Method VOLBL; Comparison With GEPOL[27,37–39†]

Protein	# Res	VOLBL	GEPOL
1eca	137	16598.5	17728.2
1nxb	62	6881.3	7385.1
1rbc	124	14332.9	15174.7
1rbe	124	14496.0	15356.6
1rbf	124	14325.3	14947.2
1rbg	124	14459.3	15181.6
1rbh	124	14423.7	15282.9
1rbi	124	14421.9	15193.6
2act	218	26071.2	28413.7
2cha	248	28038.0	30283.5
2lyz	129	15614.0	16356.4
2ptn	230	26355.1	28148.5
2rns	124	14223.3	14909.2
2sn3	51	7567.2	7971.6
3cyt	104	25291.6	26771.7
3rn3	125	14864.3	15861.3
4pti	58	6971.8	7388.5
5mbn	154	19537.9	21147.4
1arb	263	30657.3	32746.8
1cau	424	46529.0	49967.3
1cse	345	39581.0	41387.5
1ecd	136	16580.2	17470.8
1icm	131	16965.8	18363.7
1mbd	153	19473.3	20773.0
1plc	99	11758.8	11949.8
1rro	108	13239.1	13932.9
1thm	279	32501.2	33996.8
1ycc	103	13253.8	13994.2
3sdh	292	36287.3	39297.2
4gcr	174	23023.9	24040.1
5p21	165	21286.8	22523.7

†VOLBL computes volume with cusp correction for intersecting pairs only, see Immersion of Molecular Surface.

Here is a typical example in two dimensions. We consider an algorithm that needs to decide whether a point is to the right or to the left of a directed line passing through two other points. When the three points are collinear, the test is ambiguous, and let us suppose the outcome of the test is "left," maybe because of a slight bias caused by a small numerical error. When the same three points are encountered later, the test might assign an inconsistent "right" value, possibly because the points are presented to the test in a different order. This inconsistency is likely to ultimately crash the program. In principle, this problem cannot be fixed with improved numerical precision, since collinear points will always be collinear. What is needed is a decision that can be arbitrary, albeit consistent.

A popular method of battling the problem of robustness is the (actual) perturbation of atom coordinates[35,60] and/or atom radii.[61] The hope is that a small perturbation will remove all degeneracies in the data. The drawback of such perturbations is that they do not always work, and if they do work, they change the input and, thus, the output. Alternatively, one could write tests that unambiguously detect and classify degenerate cases. Such tests would have to rely on exact rather than floating-point arithmetic. This method leads to a large number of special cases, which have to be handled individually in a consistent manner. In the case of spherical balls in three dimensions, this case analysis is likely to result in complicated programming requirements.

In the computational geometry community, several methods have been suggested to cope with geometric degeneracy.[62–64] The method of choice in our implementation is the symbolic perturbation of coordinates and radii. This is referred to as SoS (for "simulation of simplicity") and described in detail in Reference 62. SoS symbolically perturbs coordinates and radii and systematically treats all special cases by a consistent reduction to the general case. We observe that only the construction of the Delaunay complex and the alpha complexes are prone to unstable behavior if presented with inaccurate numeri-

cal computation. Floating-point operations in VOLBL are solely used to compute area and volume and not to derive any decisions impacting the flow of control. The above problems of robustness and perturbation thus do not apply to VOLBL.

Immersion of Molecular Surface

The SA and the MS models are defined by the same solvent sphere rolling about the VW model. They are, therefore, combinatorially equivalent and represented by the same alpha complex. Nevertheless, the area and volume of the two models may differ significantly. For example, we can measure the area and volume variation on octanol molecule experiences during a rotation. This variation can differ by 50% between the two models.[27] Motivated by these differences, it has been suggested that the MS models represent physical/chemical phenomena more accurately than SA models.[65]

Unfortunately, the MS model suffers from an inherent geometric deficiency. Surface smoothness lacking in the SA model was probably the motivation for the development of the MS model. However, when two copies of the solvent sphere overlap in the process of reaching into a tunnel too narrow to pass through, they form cusps, which are local violations of smoothness (Fig. 3). We call these *Type I* impurities. *Type II* impurities can arise when the solvent sphere rotates about two atom balls. During this rotation, the solvent sweeps out a torus, and depending on radii and distances, this torus may intersect itself. It does so forming a spindle with reversed surface orientation. We observed that spindles in the creation of MS models of proteins occur quite frequently, and typically only small fractions of self-intersecting tori are swept out by the solvent sphere. We can either clip the molecule surface at places of self-intersection, or we can leave the surface intact and consider it an immersion rather than an embedding of an ideal surface. It is difficult to do the clipping in an algorithmically robust manner, and if we succeeded the overall smoothness of the molecular surface would be destroyed. We thus decide to ignore self-intersections and deal with the immersed surfaces. Type I impurities create self-intersections but leave the surface locally smooth. Partial spindles arising from Type II impurities violate smoothness by connecting to the rest of the surface along circular arc cusps. The numbers for MS area computed with VOLBL reflect the immersed interpretation of the surface (Table IV). An analysis of various self-intersections and an alternative smooth invariant surface can be found in Reference 66.

The meaning of the volume of an immersed molecular surface needs some explanation. The corresponding ideal surface is orientable and we measure the volume on the positive side of the immersion, which is defined as the side where all atom centers lie. We start with the volume of the SA model and subtract the volume close to the SA surface swept out by the rolling solvent sphere. A Type I impurity leads to double subtraction of the space accessible to the solvent sphere from two sides. The spindle in a Type II impurity is interpreted as negative volume because of the locally reversed surface orientation. In effect, the volume of the (partial) spindle is added to the SA volume, which compensates for a fraction of the double subtraction caused by the begining and ending positions of the rotating solvent sphere. In Table VII, the numbers computed with VOLBL reflect the immersed interpretation of the MS area and the volume computation as explained.

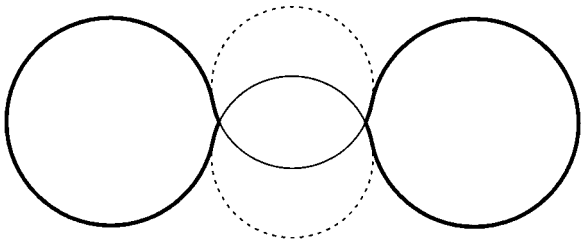

Fig. 3. Cusp in the MS model. Two solvent balls coming from two opposite sides have self-intersection.

CONCLUSIONS

This article describes an alpha shape-based algorithm for computing molecular surface area and volume for both SA and MS models. Its implementation as the program VOLBL is described in some detail in an unpublished report,[59] (but see Reference 18). It belongs to the category of analytical methods and is combinatorial in nature.[13,14] Unlike previous analytical approaches, all computations are based on the dual topological structure of the molecule, which guarantees the combinatorial correctness of the computation. For example, it does not neglect cases when more than four atoms have a common intersection, although area and volume computations of such high-order intersections are not actually performed. Efficient computation is achieved by precisely identifying atoms on the surface and their topological structure. Area and volume can be computed using the short inclusion-exclusion formula whose terms involve at most three intersecting balls at a time. The computations by DELCX and MKALF employ a symbolic perturbation[62] of the geometric data. As a consequence, our software does not suffer from a lack of robustness caused by degenerate data. We applied the method to several proteins to demonstrate both the validity and the robustness of the alpha shape-based method. In the companion article, we describe the computation of inaccessible cavities in proteins using the alpha shape method.

ACKNOWLEDGMENTS

We thank Michael Facello for the torus area formula and suggestion regarding computation of MS model

from SA model. We thank Nataraj Akkiraju, Patrick Moran, and Marcus Wagner for interesting discussions on the topic of this article and for help in the generation of two- and three-dimensional illustrations. We thank NSF Meta Center Allocation for providing computational resources. The software VOLBL is available at: http://alpha.ncsa.uiuc.edu/alpha.

REFERENCES

1. Chothia, C. The nature of the accessible and buried surfaces in proteins. J. Mol. Biol. 96:721–732, 1975.
2. Kauzmann, W. Some factors in the interpretation of protein denaturation. Advan. Protein Chem. 16:1–63, 1959.
3. Langmuir, I. "Third Colloid Symposium Monograph." New York: Chemical Catalog Co., 1925.
4. Sharp, K., Nicholls, A., Fine, R., Honig, B. Reconciling the magnitude of the microscopic and macroscopic hydrophobic effects. Science 252:106–109, 1990.
5. Richards, F.M. Areas, volumes, packing, and protein structures. Ann. Rev. Biophys. Bioeng. 6:151–176, 1977.
6. Rashin, A., Iofin, M., Honig, B. Internal cavities and buried wtares in globular proteins. Biochemistry 25:3619–3625, 1986.
7. Connolly, M. Shape complimentarity at the hemoglobin alpha1-beta1 subunit interface. Biopolymers 25:1229–1247, 1986.
8. Fersht, A. "Enzyme Structure and Mechanism." W.H. Freeman and Company, 2nd edition, 1985.
9. Freyberg, B., Richmond, T., Braun, W. Surface area effects on energy refinement of proteins. A comparative study on atomic solvation parameters. J. Mol. Biol. 233:275–292, 1993.
10. Kundrot, C., Ponder, J., Richards, F. Algorithms for calculating excluded volume and its derivatives as a function of molecular conformation and their use in energy minimization. J. Comp. Chem. 12:402–409, 1991.
11. Lee, B., Richards, F.M. The interpretation of protein structures: Estimation of static accessibility. J. Mol. Biol. 55:379–400, 1971.
12. Connolly, M. Computation of molecular volume. J. Am. Chem. Soc. 107:1118–1124, 1985.
13. Preparata, F., Shamos, M. "Computational Geometry: An Introduction." New York: Springer-Verlag, 1985.
14. Edelsbrunner, H. "Algorithms in combinatorial geometry." Berlin: Springer-Verlag, 1987.
15. Edelsbrunner, H., Kirkpatrick, D., Seidel, R. On the shape of a set of points in the plane. IEEE Trans. Inf. Theor. IT-29 4:551–559, 1983.
16. Edelsbrunner, H. The union of balls and its dual shape. Discrete Comput. Geom. 13:415–440, 1995.
17. Edelsbrunner, H., Mücke, E. Three-dimensional alpha shapes. ACM Trans. Graphics 13:43–72, 1994.
18. Edelsbrunner, H., Facello, M., Fu, P., Liang, J. Measuring proteins and voids in proteins. In: "Proc. 28th Annu. Hawaii Intl. Conf. System Sciences, Vol. 5. Los Alamitos, California: IEEE Computer Society Press, 1995:256–264.
19. Varshney, A., Brooks, F., Wright, W. Computing smooth molecular surfaces. IEEE Comput. Graphics Applications 14:19–25, 1994.
20. Shrake, A., Rupley, J. Environment and exposure to solvent of protein atoms. Lysozyme and insulin. J. Mol. Biol. 79:351–371, 1973.
21. Richards, F. The interpretation of protein structures: Total volume, group volume distributions and packing density. J. Mol. Biol. 82:1–14, 1974.
22. Richmond, T., Richards, F.M. Packing of α-helices: Geometrical constraints and contact areas. J. Mol. Biol. 119: 537–555, 1978.
23. Alden, C., Kim, S.-H. Solvent accessible surfaces of nucleicacids. J. Mol. Biol. 132:411–434, 1979.
24. Wodak, S., Janin, J. Analytical approximation to the accessible surface area of proteins. Proc. Natl. Acad. Sci. USA 77:1736–1740, 1980.
25. Muller, J. Calculation of scattering curves for macromolecules in solution and comparison with results of methods using effective atomic scattering factors. J. Appl. Cryst. 16:74–82, 1983.
26. Pavlov, M., Fedorov, B. Improved technique for calculating x-ray scattering intensity of biopolymers in solution: Evaluation of the form volume, and surface of a particle. Biopolymers 22:1507–1522, 1983.
27. Pascual-Ahuir, J., Silla, E. GEPOL: An improved description of molecular surfaces. I. Building the spherical surface set. J. Comput. Chem. 11:1047–1060, 1990.
28. Wang, H., Levinthal, C. A vectorized algorithm for calculating the accessible surface area of macromolecules. J. Comput. Chem. 12:868–871, 1991.
29. Grand, S.L., Merz, K.M. Jr. Rapid approximation to molecular surface area via the use of boolean logic and look-up tables. J. Comput. Chem. 14:349–352, 1993.
30. Connolly, T. Analytical molecular surface calculation. J. Appl. Cryst. 16:548–558, 1983.
31. Connolly, M. Molecular surface triangulation. J. Appl. Cryst. 18:499–505, 1985.
32. Richmond, T. Solvent accessible surface area and excluded volume in proteins: Analytical equations for overlapping spheres and implications for the hydrophobic effect. J. Mol. Biol. 178:63–89, 1984.
33. Gibson, K., Scheraga, H. Exact calculation of the volume and surface area of of fused hard-sphere molecules with unequal atomic radii. Mol. Phys. 62:1247–1265, 1987.
34. Gibson, K., Scheraga, H. Surface area of the intersection of three spheres with unequl radii: A simplified analytical formula. Mol. Phys. 64:641–644, 1988.
35. Perrot, G., Cheng, B., Gilson, K., Palmer, K., Nayeem, A., Maigret, B., et al. MSEED: A program for the rapid analytical determination of accessible surface areas and their derivatives. J. Comp. Chem. 13:1–11, 1992.
36. Wishart, D.L., Willard, F.R., Sykes, B. University of Alberta, Vadar Version 0.9, 1994.
37. Pacios, L. Arvomol. Quantum Chemistry Program Exchange 132, 1993.
38. Silla, E., Tuñon, I., Pascual-Ahhuir, J. GEPOL: An improved description of molecular surfaces. II. Computing the molecular area and volume. J. Comp. Chem. 12:1077–1088, 1991.
39. Pascual-Ahhuir, J., Silla, E., Tuñon, I. GEPOL: An improved description of molecular surfaces. III. A new algorithm for the computation of a solvent-excluding surface. J. Comp. Chem. 15:1127–1138, 1994.
40. Kratky, K. Intersecting disks (and spheres) and statistical mechanics. I. Mathematical basis. J. Stat. Phys. 25:619–634, 1981.
41. Finney, J. Volume occupation, environment and accessibility in proteins. The problem of the protein surface. J. Mol. Biol. 96:721–732, 1975.
42. Gellatly, B., Finney, J. Calculation of protein volumes: An alternative to the Voronoi procedure. J. Mol. Biol. 161:305–322, 1982.
43. Voronoi, G. Nouvelles applications des paramètres continus à la théorie des formes quadratiques. Premier mémoire: sur quelques propriétés de formes quadratiques positives parfaites. Journal für die Reine und Angewandte Mathematik 133:97–178, 1907 (in French).
44. David, E., David, C. Voronoi polyhedra as a tool for studying solvation structure. J. Chem. Phys. 76:4611–4614, 1982.
45. Aurenhammer, F. Voronoi diagrams—A survey of a fundamental geometric data structure. ACM Computing Surveys 23:345–405, 1991.
46. Richards, F.M. Calculation of molecular volumes and areas for structures of known geometries. Meth. Enzymol. 115: 440–464, 1985.
47. Rajan, V. Optimality of the Delaunay triangulation in r^d. Discret Comput. Geom. 12:189–202, 1994.
48. Delaunay, B. Sur la sphère vide. Izvestia Akademii Nauk SSSR, Otdelenie Matematicheskii i Estestvennyka Nauk, 7:793–800, 1934 (in French).

49. Singh, R.K., Tropsha, A., Vaisman, I.I. Delaunay tessellation of proteins: Four body nearest-neighbor propensities of amino acid residues. Comput. Aided Geom. Des. 8:123–142, 1991.
50. Zheng, W., Cho, S., Vaisman, I.I., Tropsha, A. A new approach to protein fold recognition based on Delaunay tesselation of protein structure. In: "Pacific Symposium on Biocomputing '97." World Scientific Publishing Co., 1997:486–497.
51. Munson, P.J., Singh, R.K. Statistical significance of hierarchical multi-body potentials based on Delaunay tessellation and their application in sequence-structure alignment. Protein Sci. 6:1467–1481, 1997.
52. Joe, B. Construction of three-dimensional Delaunay triangulations using local transformations. Comput. Aided Geom. Des. 8:123–142, 1991.
53. Edelsbrunner, H., Shah, N. Incremental topological flipping works for regular triangulations. In: "Proc. 8th Annu. Sympos. Comput. Geom." New York: ACM Press, 1992:43–52.
54. Munkres, J. "Elements of Algebraic Topology." Redwood City, CA: Addison-Wesley, 1984.
55. Edelsbrunner, H., Facello, M., Fu, Liang, J. On the definition and the construction of pockets in macromolecules. In: "Pacific Symposium on Biocomputing '96. World Scientific Publishing Co., 1996:272–287.
56. Kim, S., Liang, J., Barry, B.A. Chemical complementation identifies a proton acceptor for redox-active tyrosine D in photosystem II. Proc. Natl. Acad. Sci. USA 94:14406–14411, 1997.
57. McGee, M.P., Teuschler, H., Liang, J. Effective electrostatic charge of coagulation factor X in solution and on phospholipid membrane: Implications for activation mechanisms and structure-function relationships of the Gla domain. Biochem. J. In press, 1998.
58. Petitjean, M. On the analytical calculation of van der Waals surfaces and volumes: Some numerical aspects. J. Comput. Chem. 15:507–523, 1994.
59. Edelsbrunner, H., Fu, P. Measuring space filling diagrams and voids. Rept. UIUC-BI-MB-94-01, Molecular Biophysics Group, Beckman Inst. Univ. Illinois, Urbana, IL, 1994.
60. Eisenhaber, F., Argos, P. Improved strategy in analytic surface calculation for molecular systems: Handling of singularities and computational efficiency. J. Comput. Chem. 14:1272–1280, 1993.
61. Connolly, M. The molecular surface package. J. Mol. Graphics 11:139–141, 1993.
62. Edelsbrunner, H., Mücke, E. Simulation of simplicity: A technique to cope with degenerate cases in geometric algorithms. ACM Trans. Graph. 9:66–104, 1990.
63. Yap, C. Symbolic treatment of geometric degeneracies. J. Symbolic. Comput. 10:349–370, 1990.
64. Emeris, I., Canny, J. A general approach to removing geometric degeneracies. In: "Proc. 32nd Ann IEEE Sympos. Found. Comput. Sci." Los Alamitos, CA: IEEE Computer Society Press, 1991:405–413.
65. Jackson, R., Sternberg, M. Protein surface area defined. Nature 366:638–638, 1993.
66. Vorobjev, Y.N., Hermans, J. SIMS: Computation of a smooth invariant molecular surface. Biophys. J. 73:722–732, 1997.
67. Steigemann, W., Weber, E. Structure of erythrocruorin in different ligand states refined at 1.4 ang resolution. J. Mol. Biol. 127:309–338, 1979.
68. Tsernoglou, D. Structure and function of snake venom curarimimetic neurotoxins. Mol. Pharmacol. 14:710–716, 1978.
69. Varadarajan, R., Richards, F. Crystallographic structures of ribonuclease s variants with nonpolar substitution at position 13: Packing and cavities. Biochemistry 31:12315–12327, 1992.
70. Baker, E., Dodson, E. Crystallographic refinement of the structure of actinidin at 1.7 angstroms resolution by fast fourier least squares methods. Acta Crystallogr. Sect, A 36:559–572, 1980.
71. Birktoft, J., Blow, D. Structure of crystalline alpha chymotrypsin. 5. The atomic structure of tosyl alpha chymotrypsin at 2 angstrom resolution. J. Mol. Biol. 68:187–240, 1972.
72. Diamond, R. Real space refinement of the structure of hen-egg-white lysozyme. J. Mol. Biol. 82:371–391, 1974.
73. Walter, J., Steigemann, W., Singh, T., Bartunik, H., Bode, W., Huber, R. On the disordered activation domain in trypsinogen. Chemical labelling and low temperature crystallography. Acta Crystallogr., Sect. B 38:1462–1472, 1982.
74. Kim, E., Varadarajan, R., Wyckoff, H. Refinement of the crystal structure of ribonuclease s. Comparison with and between the various ribonuclease a structures. Biochemistry 31:12304–314, 1992.
75. Zhao, B. Structure of scorpion toxin variant-3 at 1.2 angstroms resolution. J. Mol. Biol. 227:239–52, 1992.
76. Takano, T., Dickerson, R. Redox conformation changes in refined tuna cytochrome c. Proc. Nat. Acad. Sci. USA 77:6371–6375, 1980.
77. Howlin, B., Moss, D., Harris, G. Segmented anisotropic refinement of bovine ribonuclease a by the application of the rigid-body/tls model. Acta Crystallogr., Sect. A 45:851–861, 1989.
78. Marquart, M., Walter, J., Deisenhofer, J., Bode, W., Huber, R. The geometry of the reactive site and of the peptide groups in trypsin, tripsinogen and its complexes with inhibitors. Acta Crystallogr., Sect. B 39:480–490, 1983.
79. Takano, T. Refinement of myoglobin and cytochrome c. Methods and applications in crystallographic computing. Hall, S.R., Hashida, T. (eds). Oxford, England: Oxford University Press: 262–272, 1984.
80. Tsunasawa, S., Masaki, T., Hirose, M. The primary structure and structural characteristics of achromobacter lyticus protease i, a lysine-specific serine protease (with appendix). J. Biol. Chem. 264:3832–3839, 1989.
81. Ko, T.-P., Ng, J.D., Day, J., Greenwood, A., McPherson, A. The 3-dimensional structures of canavalin from jack-bean (canavalia-ensiformis). Plant Physiol. 101:729–744, 1993.
82. Bode, W., Papamokos, E., Musil, D. The high-resolution x-ray crystal structure of the complex formed between subtilisin carlsberg and eglin c, an elastase inhibitor from the leech *Hirudo medicinalis*. Structural analysis, subtilisin structure and interface geometry. Eur. J. Biochem. 166:673–692, 1987.
83. Eads, J., Sacchettini, J., Kromminga, A., Gordon, J.I. *Escherichia-coli*-derived rat intestinal fatty acid binding protein with bound myristate at 1.5 angstrom resolution and i-fabp(arg106-gln) with bound oleate at 1.74 angstrom resolution. J. Biol. Chem. 268:26375–26385, 1993.
84. Phillips, S.V., Schoenborn, B. Neutron diffraction reveals oxygen-histidine hydrogen bond in oxyhemoglobin. Nature 292:81–82, 1981.
85. Guss, J., Bartunik, H., Freeman, H. Accuracy and precision in protein structure analysis—Restrained least-squares refinement of the structure of poplar plastocyanin at 1.33 angstrom resolution. Acta Crystallogr., Sect. B 48:790–811, 1992.
86. Ahmed, F. Refinement of recombinant oncomodulin at 1.30-angstrom resolution. J. Mol. Biol. 230:1216–1224, 1993.
87. Teplyakov, A., Kuranova, I., Harutyunyan, E. Crystal structure of thermitase at 14 angstroms resolution. J. Mol. Biol. 214:261–279, 1990.
88. Louie, G., Brayer, G. High-resolution refinement of yeast iso-1-cytochrome c and comparisons with other eukaryotic cytochromes c. J. Mol. Biol. 214:527–55, 1990.
89. Royer, W. Jr. High-resolution crystallographic analysis of a co-operative dimeric hemoglobin. J. Mol. Biol. 235:657–681, 1994.
90. Box, B., Lapalto, R., Nalini, V., Driessen, H., Lindey, P.F., Mahadevan, D., Blundell, T.L., Slingsby, C. X-ray analysis of beta B2-crystallin and evolution of oligomeric lens proteins. Nature 347:776–780, 1990.
91. Pai, E., Krengel, U., Petsko, G. Refined crystal structure of the triphosphate conformation of h-ras p21 at 1.35 angstroms resolution: implications for the mechanism of gtp hydrolysis. EMBO J 9:2351–9, 1990.

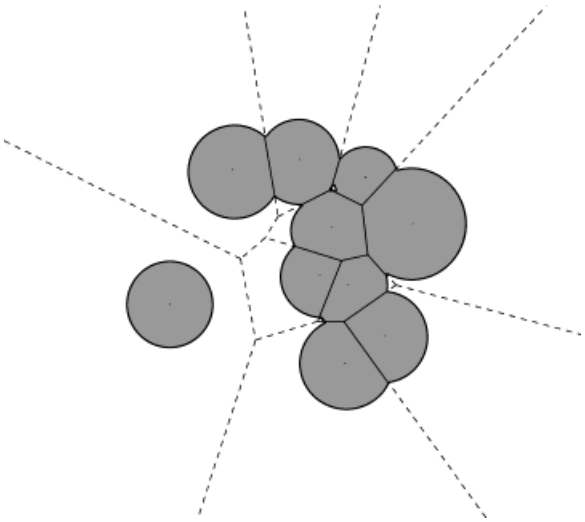

Fig. 4. The weighted Voronoi diagram (dashed lines) decomposes the molecule into convex pieces.

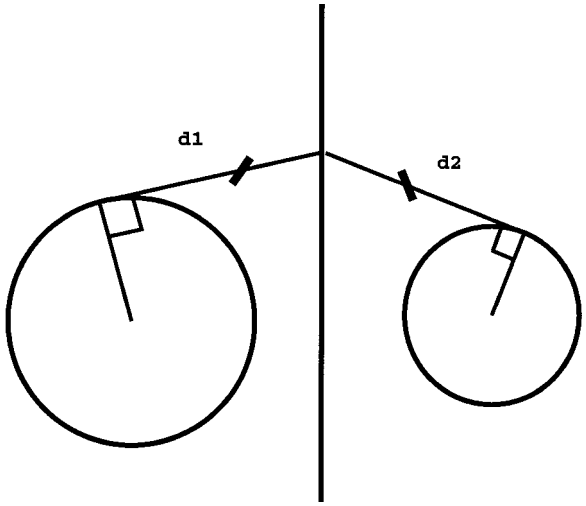

Fig. 5. The radical line is defined such that the weighted distance, i.e., the lengths of the tangent line segments to the two atoms, are equal.

APPENDIX A. GEOMETRIC AND TOPOLOGICAL CONCEPTS

A1. Voronoi Diagram

The Voronoi diagram divides the space into Voronoi regions; each region contains one atom. A Voronoi region consists of the part of space closest to the generating atom contained within. Thus, for every point inside a region its distance to the generating atom is less than (or equal to) its distance to any other atom in the molecule. See Figure 4 for a two-dimensional version, where atoms are modeled as disks.

Exactly how the space is divided up depends on what kind of distance is used. If every atom has the same van der Waals radius, we use the Euclidean distance between the point of interest and the center of the atom. As a result, the dividing plane for two equally large atoms is the bisector plane, on which every point is equidistant to the centers of both atoms. When we have different van der Waals radii for different atoms, we use the square of the length of the tangent line segment to the surface of an atom as the *weighted distance.* The dividing plane of two atoms is called the *radical plane,* which is in general different from the bisector plane of the centers, although parallel to it. Every point on the radical plane has equally long tangent line segments to both of the atoms. Figure 5 shows a radical line defined for two disks and illustrates the weighted distance to the disks. The decomposition obtained using weighted distance is called the *weighted Voronoi diagram*. Its Voronoi regions have the same properties for atoms of mixed radii as the (unweighted) Voronoi regions have for atoms of identical radii. Figure 4 illustrates the concept by superimposing atoms modeled as disks and the weighted Voronoi diagram they define. Note that the Voronoi regions neatly decompose the molecule into small convex pieces. Furthermore, the regions themselves fill space without redundant overlap.

In the general three-dimensional case, two weighted Voronoi regions either have no common intersection or they intersect in a planar facet, three regions either have no common intersection or they intersect in a common straight edge, and four regions either do not intersect or they intersect at a common vertex. Five regions do not share any common points at all. The part of an atom contained in a weighted Voronoi region is convex since the Voronoi region is convex and so is the atom ball.

A difficulty encountered by early attempts to apply Voronoi diagrams directly to molecules is dealing with the Voronoi regions that extend to infinity.[46] Whereas atoms occupy only a finite part of space, the Voronoi regions of some atoms at the surface of the molecule are infinitely large. This is a potential problem if Voronoi regions are used for computations and several heuristics for dealing with this problem have been proposed.[46,21,41,42] For example, hypothetical solvent molecules were set up around the molecule, with the sole purpose of defining positions of additional radical planes that close off Voronoi regions of atoms. As described in the next section, we use the dual of the Voronoi diagram as our combinatorial map to carry out area and volume computation, based on the atom parts contained or restricted in the weighted Voronoi regions. Together with the principle of inclusion-exclusion, this leads to an analytic method for area and volume computation, without the help of any heuristic techniques.

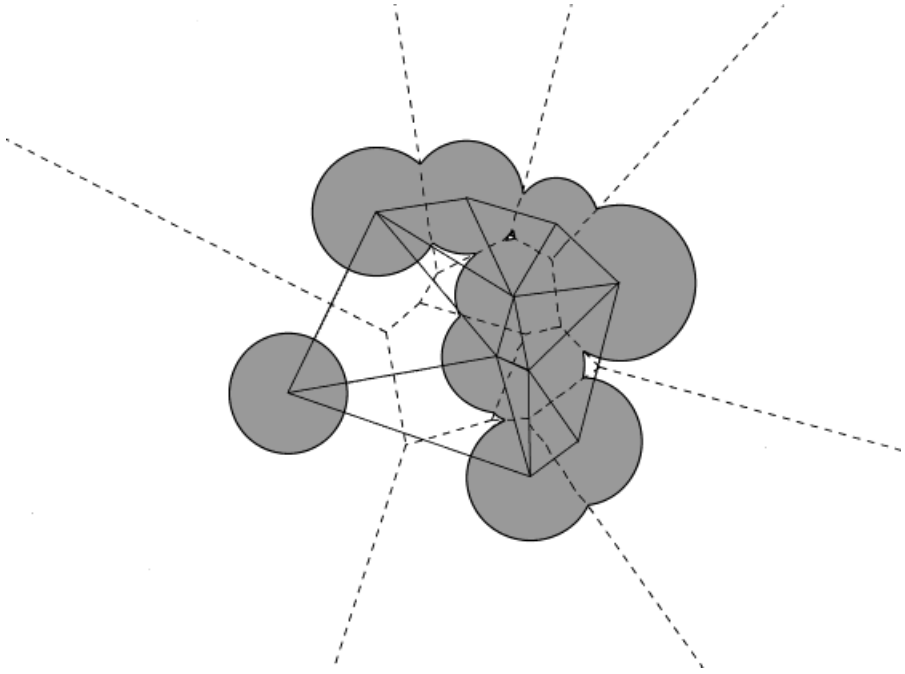

Fig. 6. Dark lines and shaded triangles display the (weighted) Delaunay complex of the centers of the atoms. The dashed lines display the (weighted) Voronoi diagram.

A2. Delaunay Complex

The problem of triangulating the atom centers might at first seem unrelated to the construction of the Voronoi diagram. The solid lines in Figure 6 show the edges of a complex that covers the convex hull of the atom centers. To describe the connection between the Voronoi diagram and a triangulating complex, we need to first define the convex hull of a set of points. Suppose we have a finite set of points in three-dimensional space, R^3, for example, the atom centers of a molecule. If we stretch a plastic wrap tightly around the points, the shape taken up by the wrap then gives the boundary of a convex body referred to as the *convex hull* of the point set. We decompose the convex hull into a collection of tetrahedra with points in the set as vertices. To cleanly fill up the convex hull, the edges of the tetrahedra are not allowed to cross or intersect the triangles, except that they may share common vertices. More formally, any two tetrahedra in the decomposition are either disjoint or they intersect in a common triangle or a common edge or a common vertex. Such a decomposition is called a *simplicial complex*. The complex triangulates the set of points. In R^2, the tetrahedra are reduced to triangles (Fig. 6). A set of points can be triangulated in many ways. The complex shown in Figure 6 is a well-known one, called the Delaunay complex or Delaunay triangulation. It has many useful geometric properties (see, e.g., Reference 47), and it reflects the boundary overlap among the Voronoi regions. We described in Theory and Algorithms a rule to obtain the Delaunay complex from the Voronoi diagram. Observe that the rule guarantees that if an edge belongs to the complex then its endpoints are vertices in the complex. Similarly, if a triangle belongs to the complex then so do its edges, and if a tetrahedron belongs to a complex then so do its triangles.

The duality between the Delaunay complex and the Voronoi diagram is reflected in a number of aspects. In R^3, each vertex, edge, triangle, and tetrahedron in the Delaunay complex corresponds to a Voronoi region, facet, edge, or vertex in the Voronoi diagram. Similarly in R^2, each vertex, edge, and triangle in the Delaunay complex corresponds to a Voronoi region, edge, or vertex in the Voronoi diagram. (See Figure 6 for an illustration of the two-dimensional case, where the Delaunay complex and the Voronoi diagram are superimposed.) An important consequence of the duality is that algorithms for Delaunay complexes are meaningful for Voronoi diagrams and vice versa. In particular, it is easier to design a robust algorithm for constructing Delaunay complexes than for constructing Voronoi diagrams. The main reason is that the Delaunay complex comprises no new geometric information and all edges, triangles, and tetrahedra can be stored combinatorially as pairs, triplets, and quadruplets of vertex indices. In contrast, the Voronoi diagram contains vertices that are not part of the input data. The Delaunay complex has an added advantage in that it lives in a bounded space and does not extend to infinity.

The method we use to compute the Delaunay complex of a set of spherical balls is based on the notion of flipping.[52,53,17] This is implemented in the DELCX program. The most common type of flip in R^2 changes the diagonal of a convex quadrilateral.

Before the flip the quadrilateral is decomposed into two triangles sharing a diagonal; after the flip it is decomposed into the two triangles sharing the other diagonal. There are two other types of flips. One adds a point in the middle of a triangle and decomposes the triangle into three smaller ones, the other removes a vertex common to three triangles and replaces them by their union, which is again a triangle. In R^3, there are four types of flips. An edge shared by three tetrahedra can be replaced by the triangle shared by two tetrahedra occupying the same part of space. Inversely, a triangle shared by two tetrahedra can be replaced by the edge shared by three tetrahedra. A single tetrahedron can be decomposed into four by adding a new vertex inside. Inversely, a vertex shared by four tetrahedra can be removed replacing the four by their union, which is again a tetrahedron.

The program DELCX adds one point at a time via a flip that decomposes the containing tetrahedron into four. Successive flips are used to transform the neighborhood of the new point into a decomposition with Delaunay tetrahedra.[52,53] For molecules, this algorithm has time-complexity O(n log n). This is a consequence of the spatial distribution of atoms in molecules, which typically form a dense arrangement of balls. All atoms have bond lengths of roughly the same length and the distribution is more or less of uniform density. For such a spatial arrangement, the number of tetrahedra, triangles, edges, and vertices in the Delaunay complex is O(n) and the required time is O(n log n).

A3. Simplicial Complexes

We are interested in the Voronoi decompositions of the molecule rather than the decomposition of the entire space. Similarly, we are not just interested in the Delaunay complex of the molecular convex hull but rather the part that corresponds to the molecule. To understand how to obtain information from the Delaunay complex about the actual molecule, we first need to describe a few topological concepts, which can be found in introductory texts on topology (see, e.g., Reference 54).

Topology creates a unified language and notation by calling a vertex a *0-simplex,* an edge a *1-simplex,* a triangle a *2-simplex,* and a solid tetrahedra a *3-simplex.* The integer number indicates the intrinsic dimension. Examples are shown in Figure 7A. Observe that the boundary of a simplex consists of other simplices, albeit their dimensions are lower. These lower-dimensional simplices are the *faces* of the original simplex.

Complicated geometric objects can be built from a collection of simplices. The goal is to construct the object in an organized fashion. This is achieved by adhering to the following rules:

(i) for every simplex used, its faces are also part of the construction, and

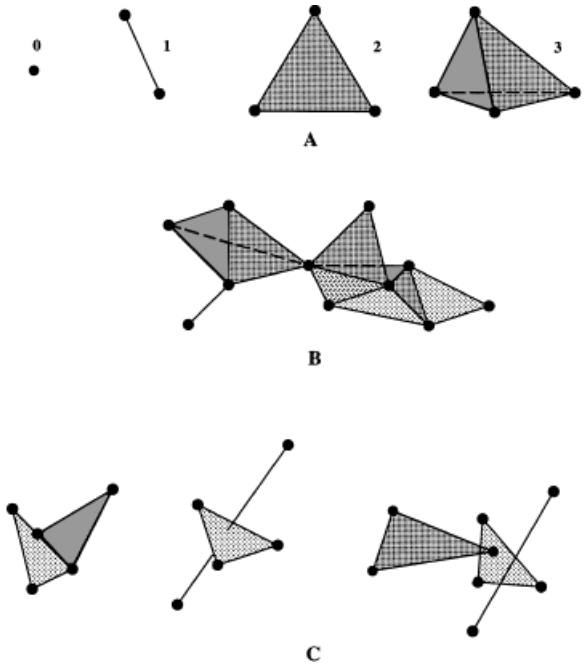

Fig. 7. (**A**) A 0-simplex is a vertex, a 1-simplex is an edge, a 2-simplex is a triangle, and a 3-simplex is a tetrahedron. (**B**) A collection of simplices that fit together nicely in three-dimensional space. (**C**) Intersection patterns among simplices that are not allowed in a complex.

(ii) the common intersection of any two simplices is either empty or a face of both simplices.

Figure 7B and C illustrates these ideas. If the above two rules are followed, the resulting object is called a *simplicial complex.* We have already seen an example of such a complex, namely the Delaunay complex of a molecule. It contains a wealth of combinatorial information about the molecule.

A4. Alpha Complexes and Alpha Shapes

To explain the idea behind the alpha shape, we first ignore the differences in van der Waals radii among atoms and assume all have the same radius. For all the atoms in this peculiar molecule, we start to grow balls simultaneously from each atom center by gradually increasing the uniform radius, α. A ball grows only inside its own Voronoi region and is clipped when it reaches the boundary of this region. A simplex is collected at the moment the clipped balls growing from its vertices have a common boundary intersection.

We have the following scenario. At the beginning when radius is 0, we only have vertices in our collection, and we take the atom centers as the first elements to appear in our sequence of simplices. All vertices appear simultaneously. Because the balls gradually grow they will eventually overlap. At the moment when the boundaries of two clipped balls overlap, we chronologically mark the corresponding edge in the Delaunay complex, and add it at the end of the evolving sequence. When the

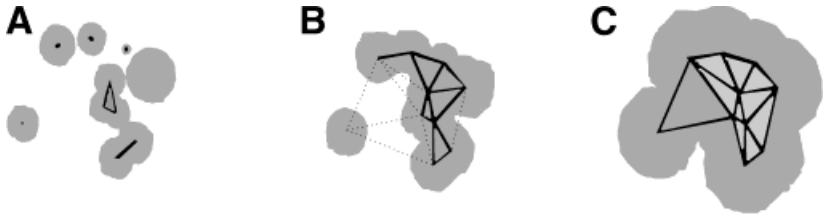

Fig. 8. (**A**) The alpha complex for the small value of alpha consists mostly of vertices, together with four edges and one triangle. (**B**) The alpha complex for the medium value of alpha consists of two components, one just a vertex and the other consisting of quite a few triangles, edges, and vertices. It contains the complex in (**A**) as a subcomplex (**C**). The alpha complex for the large value of alpha is connected and contains the other alpha complexes as subcomplexes.

boundaries of three clipped balls grow to overlap, we mark the corresponding triangle in the Delaunay complex and add it to the sequence. We do the same for the solid tetrahedra whenever the boundaries of four clipped balls overlap. When the balls are grown large enough, all the simplices in the Delaunay complex will have been put in the sequence. Thus, we have organized all the simplices into a sequence. In topology, this sequence is called a *filter* of the simplicial complex. The filter has an important property. If we sequentially choose any number of simplices from the beginning of the sequence, we obtain a collection of simplices that itself forms a complex. It is a *subcomplex* of the Delaunay complex. The sequence of such subcomplexes is called a *filtration* of the Delaunay complex.

Note that when two balls grow, their bounding spheres intersect in a circle that sweeps out the bisector plane. A piece of this plane is found as a two-dimensional facet in the Voronoi diagram. Now we consider atoms of different sizes. We assign the van der Waals radius of the associated atom as the initial radius r_0 to each ball. We grow or shrink the ball by changing the α parameter: the actual radius is

$$r_\alpha = \sqrt{r_0^2 + \alpha^2}.$$

For increasing α the ball grows and for decreasing α the ball shrinks until it vanishes when $\alpha^2 = -r_0^2$. This would never be the case if we chose α from the set of real numbers. To avoid this technical difficulty, we choose α^2 from the set of real numbers, positive and negative, which really means we choose α from the set of non-negative reals or positive multiples of the imaginary unit, $\sqrt{-1}$. When $\alpha = 0$, we have the actual size of the molecule. Note that the particular way a ball grows under this formula dictates that the weighted Voronoi diagram, and hence the Delaunay complex, stay the same at all times when α changes value.[17] By growing the balls in this fashion we again obtain a sequence of the Delaunay simplices, i.e., the filter.

If we increase α from its least possible value, we can imagine an index moving along the filter from its start. When we stop at a certain value, all simplices to the left of the index have shown up and form a simplicial complex. The corresponding ball diagram at the moment is characterized by the particular α value, which controls the ball size. The simplicial complex associated with an α value is a subcomplex of the Delaunay complex and is referred to as the *alpha complex*.[15,17] The *alpha shape* is the part of space covered by simplices in the alpha complex. Figure 8 shows the alpha complex of the two-dimensional molecule in Figures 4 and 6 for a small, medium, and large value of α. Because of the filter property, simplices in an alpha complex for a smaller value of α are present in an alpha complex of a larger value of α. As a result, the alpha complex for a smaller value of α is always a subcomplex of one for a larger value of α, and both are subcomplexes of the Delaunay complex. Furthermore, the number of possible alpha complexes for a molecule cannot exceed the number of simplices in the Delaunay complexes.

The combinatorial equivalence between the alpha complex and the corresponding Voronoi decomposition of the union of balls is most obvious from the definition: each simplex indicates a collection of clipped balls with a non-empty common intersection. The topological correspondence between the molecule and the alpha complex (for $\alpha = 0$) can be seen from Figure 8. Consider, for example, the tiny hole in the molecule represented by the disk union in Figure 8B. It corresponds to a much larger triangular hole in the alpha complex. If the atom sizes were a little larger, such as in C, where that specific hole has disappeared, the planar triangle would have been added so as to fill the hole in the alpha complex. As illustrated, each component of the union of disks contains a component of the alpha complex, and each hole of the union of disks is contained in a hole of the alpha complex. Mathematically, there is a homotopy equivalence between the molecule and the alpha complex (for $\alpha = 0$).[16] One characteristic of combinatorics is that changes occur in discrete steps, such that the actual size of the hole has no direct influence on the nature of the alpha complex. Taking advantage of this topological correspondence, we can locate all voids inside a protein, regardless of their sizes. We can also identify atoms facing outside with precision. Void or inaccessible cavity computations will be explained in the companion article. The third correspondence between the molecule and its alpha complex is the capability to obtain area and volume information directly from the alpha complex without explicitly constructing the geometric model of the molecule. As an application, we see in this article and the companion article how the simplices in the alpha complex can be translated into a combinatorial expressions for the volume and surface area of a molecule and its cavities.

APPENDIX B. COMPUTATIONAL ASPECTS

B1. Direct Inclusion-Exclusion

As to reducing the redundant terms in the *direct inclusion-exclusion formula*, a similar but weaker result has been discovered for the earlier two-dimensional case.[40] Kratky observed that the common intersection of four or more circular disks can be reduced to a signed sum of lower order intersections. Successive application of this idea eventually leads to a formula where each term is the intersection of at most three disks. This formula may still contain redundant terms and will generally be longer than the formula obtained from the alpha complex. Kratky's idea has been applied to three dimensions without proof.[33]

In this context, it is worth mentioning that the intersections of up to four atom balls derived from the alpha complex all have a uniform structure. This simplifies the necessary analytic computation of volume and area for such small groups of atoms. To explain the uniformity, consider a tetrahedron in the alpha complex whose vertices are the centers of atom balls b_1, b_2, b_3, and b_4. First, the intersection of the balls is non-empty. Second, the common intersection of any three of the four balls is non-empty and not contained in the fourth ball. Third, the common intersection of any two of the four balls is non-empty and not contained in the union of the other two balls. Finally, no ball is contained in the union of the other three balls. Such a configuration is referred to as an *independent* collection of balls. The reductions described earlier are possible because collections of five or more spherical balls in three-dimensional space cannot be independent and because every non-independent collection can be reduced to a signed combination of smaller collections. This also implies that a formula obtained by following the ideas of Kratky can still be further reduced until all terms correspond to independent collections.

B2. Short Inclusion-Exclusion

Although the inclusion-exclusion formula obtained from the alpha complex contains only independent terms and is therefore minimal, it is possible to find even shorter expressions of area and volume if fractional coefficients are used in the formulas. We can use the angles at the atom centers relative to its neighbors in the alpha complex as coefficients for that purpose. All angles are measured as fractions of circles or spheres and are thus automatically normalized between 0 and 1. This is what we refer to as the *short inclusion-exclusion method*. It expresses the surface area as a sum of areas of intersections of at most three balls, each with an angle coefficient. A similar approach is taken in summing the volume, except that the total volume of all tetrahedra in the alpha complex needs to be added to the sum of the intersections. Tetrahedra volumes are significantly easier to compute than volumes of the intersections of four balls, which leads to improved running-time even in the case of volume. The short inclusion-exclusion method is important for practical computation.

Rather than describing the short formula in detail we refer the reader to Edelsbrunner[16] and present a small two-dimensional example. Figure 2B illustrates the method in two dimensions. In this case, the alpha complex consists of a single triangle, four edges, and four vertices. Let ϕ_2, ϕ_3, ϕ_4 be the outside angles of the triangle. Then the area of the disk union is

$$A_{\text{total}} = (1 \cdot A_1 + \phi_2 \cdot A_2 + \phi_3 \cdot A_3 + \phi_4 \cdot A_4) - \left(1 \cdot A_{12} + \frac{1}{2} \cdot A_{23} + \frac{1}{2} A_{24} + \frac{1}{2} A_{34}\right) + A$$

where A is the area of the triangle. In general, A is the total area of all triangles in the alpha complex, or in three dimensions it is the total volume of all tetrahedra.

B3. Algorithms

In this description, we use the following notation: κ for the alpha complex, σ for a simplex in κ, i for a vertex, ij for an edge, ijk for a triangle, and ijkl for a tetrahedron. The algorithm expressing the direct inclusion-exclusion method can be written as:

V := A := 0.0;

for each $\sigma \in \kappa$ do

if σ is a vertex i then V := V + vol(b_i);
A := A + area(b_i) endif;

if σ is an edge ij then V := V − vol($b_i \cap b_j$);
A := A − area ($b_i \cap b_j$) endif;

if σ is a triangle ijk then V := V
+ vol($b_i \cap b_j \cap b_k$); A := A
+ area($b_i \cap b_j \cap b_k$) endif;

if σ is a tetrahedron ijkl then V := V
− vol($b_i \cap b_j \cap b_k \cap b_l$); A := A
− area($b_i \cap b_j \cap b_k \cap b_l$) endif

endfor.

Here, vol() and area() are metric functions for volume and area computations of the intersection of up to four balls. As mentioned earlier, all intersections are of a uniform type; namely, the atom balls involved are independent.

For the short inclusion-exclusion method, we divide our computations into three parts: void computation, shape computation, and outside-fringe computation. *Voids* here are defined in strictly topological sense; that is, they are cavities buried inside the molecule that have no open outlets to connect them to the outside. In void computation, the volume of a

void is computed by first measuring the volume of the corresponding void in the alpha complex, then measuring the volume and area of the atom balls that reach into this void in the complex. Volume of the complex void minus the volume covered by the reaching-in balls gives the volume of the actual void in the molecule. More details of void computation can be found in the companion article (see also Reference 18). Shape computation is straightforward: it sums the volume over all the tetrahedra found in the alpha complex.

The *outside-fringe* is the part of the molecule that lies outside the alpha complex. It is measured by the short inclusion-exclusion method, which was illustrated by our second example earlier. The algorithm can be summarized as:

$V := A := 0.0;$

for each σ on the outside boundary of κ do

if σ is a vertex i then $V := V + \phi_\sigma \cdot \mathrm{vol}(b_i)$;

$A := A + \phi_\sigma \cdot \mathrm{area}(b_i)$ endif;

if σ is an edge ij then $V := V - \phi_\sigma \cdot \mathrm{vol}(b_i \cap b_j)$;

$A := A - \phi_\sigma \cdot \mathrm{area}(b_i \cap b_j)$ endif;

if σ is a triangle ijk then $V := V + \phi_\sigma \cdot \mathrm{vol}(b_i \cap b_j \cap b_k)$; $A := A + \phi_\sigma \cdot \mathrm{area}(b_i \cap b_j \cap b_k)$ endif

endfor.

For a vertex σ, ϕ_σ is the solid angle at σ outside the alpha complex. For an edge σ, ϕ_σ is the dihedral angle at σ outside κ. Finally, for a triangle σ, ϕ_σ is 1 if both sides of σ lie on the outside and ½ if only one side lies on the outside of κ.

B4. Area and Volume of MS Model

Here, we explain the computation of MS area and volume in more detail. Each sphere patch of the SA model corresponds to a somewhat smaller but otherwise identical sphere patch in the MS model. Each circular arc where two intersecting atoms meet in the SA model corresponds to a torus patch in the MS model. This torus patch is swept out by the solvent sphere as its center moves along the circular arc. Each corner point of the SA model where three atom balls meet corresponds to an inverse sphere patch that lies on the surface of the solvent sphere, whose center is the corner point. Figure 9 illustrates the relationship between the MS and the SA model in two dimensions, and it indicates how the metric sizes of the MS patches can be computed from the SA model (see Reference 18).

The ball radius of an atom in the SA model, r_{SA}, is the sum of its van der Waals radius r_{VW} and the radius of the solvent sphere, r_s. We shrink the SA model by excluding all volume that can be reached by a copy of the solvent sphere with a center on the SA surface. The effect of this shrinking process is different for the sphere patches, the circular arcs, and the corner points of the SA model. A sphere patch shrinks to radius r_{VW} towards its center; this gives the convex sphere patches of the MS model. A circular arc grows into a torus patch, which is a saddle-shaped patch. In two dimensions, the torus patch becomes an arc of a circle outside the MS model (see Fig. 9). A corner point at the intersection of three spheres in the SA model grows into a triangular patch on the solvent sphere centered at the corner point.

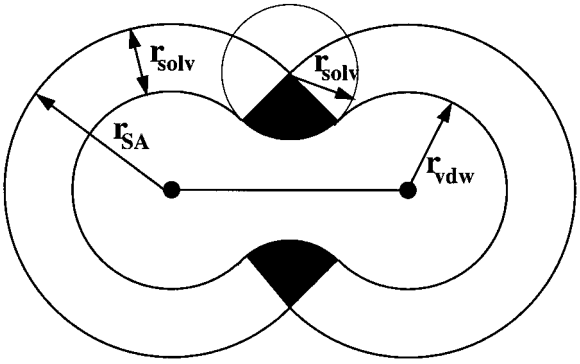

Fig. 9. Correspondence between the molecular surface (MS) and the solvent accessible (SA) model of a molecule; r_s is the radius of the solvent probe sphere, r_{SA} and r_{VW} are the SA and VW radii, respectively.

Measuring the MS model requires the computation of area and volume of various basic geometric pieces. For example, the formula for computing the fraction of the torus swept out by a revolving circular arc bounding the disk sector shown in black in Figure 9 can be obtained by using the following formula, which measures the part of the torus on one side of the (radical) plane through the circular arc:

$$\mathrm{Area} = 2\pi \cdot r_s(r_d \cdot \theta - r_s \cdot \sin\theta)$$

where r_d is the radius of the circular arc in the SA model, which is also the center circle of the torus, and θ is the angle between the plane containing the circular arc and the line from the edge of the torus to the center of the corresponding solvent sphere. Note that the above formula measures the area for a complete revolution of the arc. In general, we have partial revolutions and the area is the appropriate fraction of the complete revolution. The following formula computes the volume of the same piece of solid torus swept out by the disk sector.

$$\mathrm{Volume} = \pi \cdot r_s^2\left(r_d \cdot \theta - \frac{2}{3} r_s \cdot \sin\theta\right)$$

Formulas for other basic geometric pieces, such as ball wedges, ball sectors, sphere caps, etc., can be found in Reference 59.